DOI: 10.1002/anie.201003952

Nanowires

Controlled Colloidal Growth of Ultrathin Single-Crystal ZnS Nanowires with a Magic-Size Diameter**

*Zhengtao Deng, Hao Yan, and Yan Liu**

Semiconductor nanowires (NWs) with ultrathin diameter below the exciton Bohr radius, especially those with magic-size (i.e., less than 2 nm) diameter, have attracted significant interest in the past few years because of their predicted unique quantum confinement effects, quantum conductance, ballistic conduction, low thermal conductivity, increased surface area properties, and potential applications in thermoelectric devices, sensors, catalysts, and other nanodevices.[1–12] Spherical magic-size semiconductor clusters (or ultrasmall nanocrystals) with a well-defined number of atoms have been extensively prepared by various techniques.[13–16] However, ultrathin semiconductor NWs with magic-size diameter have been difficult to achieve previously.[2]

Zinc sulfide (ZnS), an important semiconductor material with a direct band gap of 3.6 eV at room temperature and a large exciton binding energy of 40 meV, is widely used in lasers, electroluminescent devices, flat panel displays, field emitters, infrared windows, and UV-light detectors.[17,18] The synthesis methods for ZnS NWs have been intensively studied in the past few years.[19–26] For example, Lieber and coworkers[25] developed a gold nanocluster-catalyzed single-source molecular precursor method to prepare ZnS NWs with 17 nm diameter. Yu et al.[27] synthesized uniform ZnS nanorods with diameter of approximately 5 nm and length of around 21 nm by a colloidal chemical synthetic route, which represents an exciting step towards the synthesis of ultrathin semiconducting nanowires. To the best of our knowledge, there has been no report describing high quality ZnS NWs with diameters below 2 nm.

Herein, we report a simple, fast, green, and catalyst-free colloidal method for the synthesis of single-crystal ZnS NWs with diameter down to 1.2 nm, which is well below the exciton Bohr radius of ZnS (2.5 nm). Unusual properties related to the unique nature of the ultrathin ZnS NWs, such as large blue-shifted UV/Vis exciton absorption spectra, surface defect state dominant photoluminescence emission spectra, and geometry-related XRD pattern, were observed.

The current synthetic technique for ultrathin NWs was developed from the green phosphine-free colloidal method for the synthesis of spherical semiconductor nanocrystals.[28,29] Briefly, ultrathin NWs were grown after injecting sulfur oleylamine (OAm) precursor into Zn^{2+}–OAm precursor in presence of 1-dodecanethiol (DDT). Details are described in the Supporting Information. It is worth noting that we used green and air-stable zinc nitrate salt as the zinc source for the ZnS NWs synthesis. This precursor is chemically more stable than the toxic and flammable diethylzinc used in the previous study.[27]

Transmission electron microscopy (TEM) images (Figure 1a and Figure S1 in the Supporting Information) show the formation of NWs with large aspect ratio and lengths of up to 250 nm. The contrast of the TEM images is low, possibly because of the extremely small diameter of the NWs. To obtain better microscopic images, we used high-angle annular dark-field scanning transmission electron microscopy (HAADF-STEM) to image these NWs, which gave much higher image contrast (Figure 1b–d and Figure S2). The STEM images also provide direct evidence for the formation of higher-order structures. When the sample was dried on the TEM grid, it is found that the NWs tend to align parallel to each other to form closely packed array structures (Figure 1c), which was confirmed by fast Fourier transform (FFT, Figure 1c inset). In addition, overlapping layers of arrays were also observed (Figure 1d). The formation of these ordered arrays provides further evidence that the NWs have highly uniform diameters.

High-resolution TEM (HRTEM) images (Figure 1e–g and Figure S3) revealed that the NWs have a uniform and narrow diameter of 1.2 nm. The NWs have preferred crystallographic orientation of [111]. The well-resolved lattice structure of individual NWs (Figure 1f,g) indicates that the NWs are single-crystalline. The distinct lattice spacings were measured to be approximately 0.31 nm, corresponding to the [111] plane spacing of cubic zinc blende (ZB) phase of ZnS (cell constant $a = 5.345$ Å; JCPDS Card No. 80-0020). This result also indicates that the NWs grow along the [111] direction. It should be noted that special care is needed to image these ultrathin NWs because they tended to break into spherical nanocrystals if they were exposed in a strong electron beam for a few minutes (see Figure S4). The powder X-ray diffraction (XRD) pattern of the NWs (Figure 2a) can be indexed to a cubic ZB phase, which is consistent with the HRTEM observations. The narrow (111) peak is due to the very large size (ca. 250 nm) in the length direction, while the

[*] Dr. Z. Deng, Prof. Dr. H. Yan, Prof. Dr. Y. Liu
Department of Chemistry and Biochemistry
and
The Biodesign Institute, Arizona State University
Tempe, AZ 85287 (USA)
Fax: (+1) 480-727-2378
E-mail: yan_liu@asu.edu

[**] This research was supported in part by grants from the ARO, ONR, NSF, DOE, and NIH to Y.L. and H.Y., and from the Sloan Research Foundation to H.Y.; Y.L. and H.Y. were supported as part of the Center for Bio-Inspired Solar Fuel Production, an Energy Frontier Research Center funded by the U.S. Department of Energy, Office of Science, Office of Basic Energy Sciences under award number DE-SC0001016.

Supporting information for this article is available on the WWW under http://dx.doi.org/10.1002/anie.201003952.

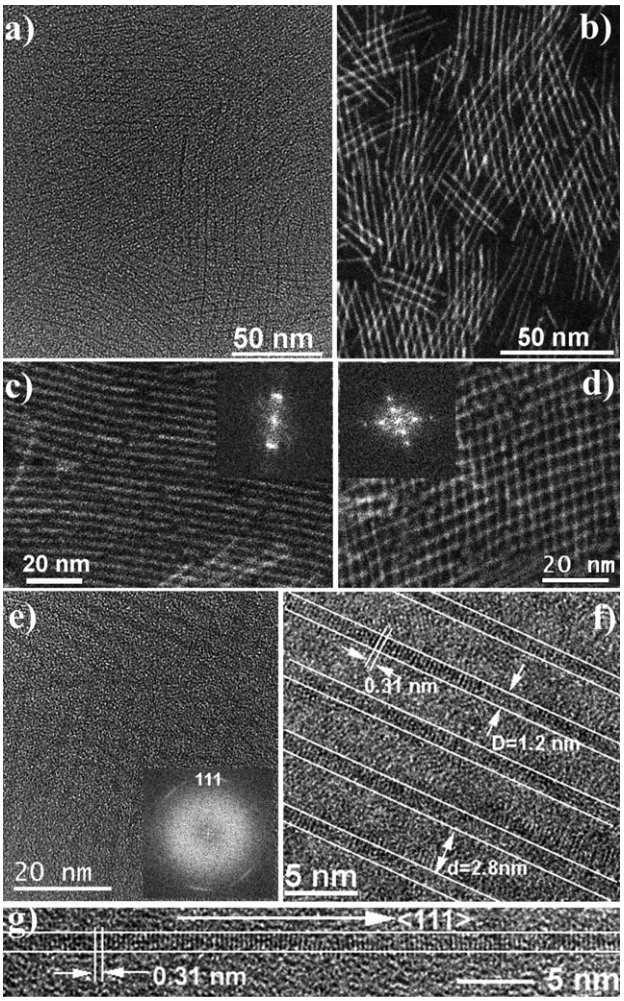

Figure 1. a) TEM image of the magic-size ZnS nanowires. b–d) HAADF-STEM images of NWs; insets in (c,d) are their corresponding fast Fourier transform (FFT) images, showing the formation of superlattice structures. e–g) HRTEM images of NWs; inset in (e) shows the corresponding FFT image of (e); the white lines in (f,g) label the boundary of individual NWs, showing the formation of single crystal NWs with diameter of 1.2 nm.

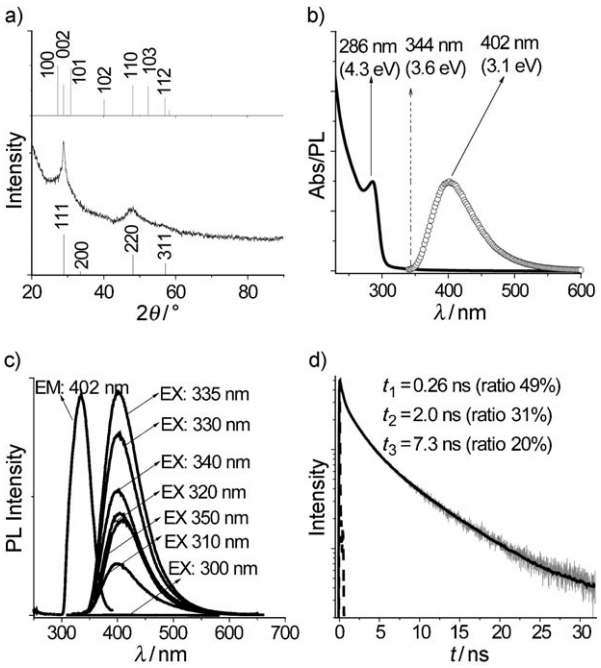

Figure 2. a) XRD pattern of the magic-size ZnS nanowires and reference patterns (vertical lines) from JCPDS card No. 80-0020 (zinc blende, bottom) and JCPDS card No. 80-0007 (wurtzite, top). b) Room-temperature UV/Vis absorption (solid black line) and photoluminescence spectra (circles) of NWs. The dashed vertical arrow points to the bulk ZnS band gap. c) PL excitation and emission spectra monitored at different wavelengths; Em: 402 nm, emission monitored at 402 nm; Ex: 335 nm, excitation wavelength at 335 nm. d) Room-temperature PL emission decay curve (gray) of the NWs with 402 nm emission and 355 nm excitation; the solid black line is the corresponding fitting curve; and the dashed line is the instrument response function curve.

broad (220) peak is due to the very small size (ca. 1.2 nm) in the width direction. The (311) peak intensity decreased significantly relative to bulk ZB phase ZnS, indicating the preferred crystallographic orientation of the product. These unusual characteristics of the XRD pattern are consistent with the unique geometry of the ultrathin NWs, which is expected to exhibit overlap of extremely broad and sharp features due to extreme difference of coherence lengths along different crystallographic axes.[2] The energy-dispersive X-ray spectroscopy (EDS) spectrum (Figure S5) suggests that the NWs are composed of Zn and S. Quantitative EDS spectrum shows an atom ratio of Zn:S is 49.1:50.9, which is close to 1:1 and confirms the composition of the as-synthesized product is ZnS.

The UV/Vis absorption and photoluminescence (PL) emission spectra of the ultrathin ZnS NWs dispersed in hexane were measured at room temperature (Figure 2b). The distinct peak at $\lambda = 286$ nm (4.34 eV) is due to the first exciton absorption band of the ultrathin NWs. The large blue-shift (ca. 0.74 eV) relative to the bulk zinc blende ZnS band gap (3.60 eV) indicates the existence of very strong two-dimensional quantum confinement effect,[12] which is due to the ultrathin diameter of the NWs. The sharp absorption peak also indicates that the NWs are uniform in diameter, which is consistent with the TEM and STEM results. The PL emission spectrum exhibits a broad band peak at $\lambda = 402$ nm (3.08 eV) and a full width at half maximum of approximately 0.6 eV, which could be assigned to the surface states.[30] To further reveal the PL properties of the sample, the emission spectra were collected with the excitation wavelength varied in discrete steps in the range from 300 to 350 nm (Figure 2c). The emission peak at 402 nm (3.08 eV) showed a slight red shift (< 5 nm) with longer excitation wavelengths, reflecting an intrinsic surface-related states of the NWs. The excitation spectrum with emission monitored at 402 nm revealed a narrow PLE peak centered at $\lambda = 335$ nm (3.70 eV), that is more than 0.64 eV away from the exciton absorption peak. This result further suggests that the emission originates from the surface-related states, not from the direct band-gap excitation. The magic-size diameter of the NWs causes a significant increase of surface-to-volume ratio, which leads to the increase in amount of surface states. The PL quantum

yield of the NWs was measured to be around 0.08, which is higher than the surface-related PL emission of ZnS nanocrystals (0.014) and nanorods (0.011) reported in the previous study.[27] The room-temperature time-resolved emission decay curve (Figure 2d) at 402 nm fits well to a triexponential function with three characteristic time constants 0.26 ns (49%), 2.0 ns (31%), and 7.3 ns (20%). The amplitude weighed average decay time is 2.2 ns.

The exact mechanism of growth of ultrathin ZnS nanowires is still largely unknown. We postulate that the formation of ultrathin ZnS nanowires may be attributed to a ligand-controlled oriented-attachment mechanism, as demonstrated previously for the cubic (ZB) ZnS nanorods synthesized with OAm as the capping ligand.[27] Our ultrasmall ZnS nanocrystals could coalesce during the oriented attachment process to form the ultrathin ZnS nanowires with their (111) planes perfectly aligned. This behavior might be because the capping ligands (OAm and DDT) bind stronger to planes such as {220} and {100}, but more weakly to the {111} plane.[2,8,27,31] This preference is evidenced by the ⟨111⟩ growth direction of the nanowires shown in the HRTEM image (Figure 1g). We found that with OAm but without DDT, short nanorods and spherical nanocrystals (Figure 3a) were obtained. Moreover, if overdosed DDT was used (molar ratio of DDT:Zn ≈ 30:1, instead of around 5:1), the products were short, branched, or wormlike nanorods (Figure 3b). OAm has a double bond in the middle of the chain, which prevents the formation of ordered monolayers stabilized by van der Waals interactions,[2] whereas DDT, without the double bond, is likely to form more closely packed monolayers. DDT may bind stronger on the sides of the ZnS nanowires than does OAm, which will greatly reduce the surface energy of the side planes (such as {220}), thus keeping it from growing wider. As a result, ultrathin nanowires with large aspect ratios were obtained.

Temperature is also important for the ultrathin NW synthesis. When the synthesis was performed at the higher temperature of 260 °C, instead of 230 °C, only large (ca. 6 nm) spherical nanocrystals were produced (Figure 3c). Finally, if the ultrathin NWs were aged at 230 °C for a longer time (from 3 to 15 min), the NWs became thicker and shorter nanorods: the average length shrunk from 250 to 40 nm; the diameter grew from 1.2 to 3.0 nm; and the average aspect ratio of NWs decreased from about 208 to 13 (Figure 3d). The volume of the NWs remained constant at about 282 nm^3, which implies that the shape evolution is by a diffusion-controlled one-dimensional to two-dimensional intraparticle ripening as a result of the extremely high overall chemical potential of the NWs shape. This result is consistent with the temporal shape evolution of CdSe nanorods previously observed.[32] The above results indicate that high quality magic-size NWs can be synthesized by using the optimized experimental parameters in a well-controlled manner. The as-synthesized ultrathin NWs are stable in hexane at room temperature for months if purified from the reaction mixture.

The absorption and emission spectra of the 3 nm diameter ZnS nanorods are shown in Figure S6. Relative to the 1.2 nm diameter ZnS nanowire, the absorption peak red shifts from $\lambda = 286$ nm to $\lambda = 295$ nm (0.14 eV shift), and the emission peak shows only a slight shift from $\lambda = 402$ nm to $\lambda = 404$ nm (0.01 eV shift). This observation is consistent with the assignment of the emission to surface states, which is expected to experience less quantum confinement effect than the exciton bandgap.

In summary, we have developed a facile colloidal chemistry for synthesis of ultrathin ZnS nanowires with magic-size diameter of 1.2 nm. Strong quantum confinement effects related to the unique nature of these ultrathin NWs were observed. We believe these ultrathin NWs could find broad use in sensors, photodetectors, host materials for diluted magnetic semiconductors (DMSs), and other nanodevice applications. These ultrathin NWs may also be used as a model to study the strong quantum confinement effect in a one-dimensional system. By choosing appropriate precursors and synthetic parameters, it is reasonable to expect that the present method could be extended to the synthesis of other ultrathin semiconductor NWs with magic-size diameter.

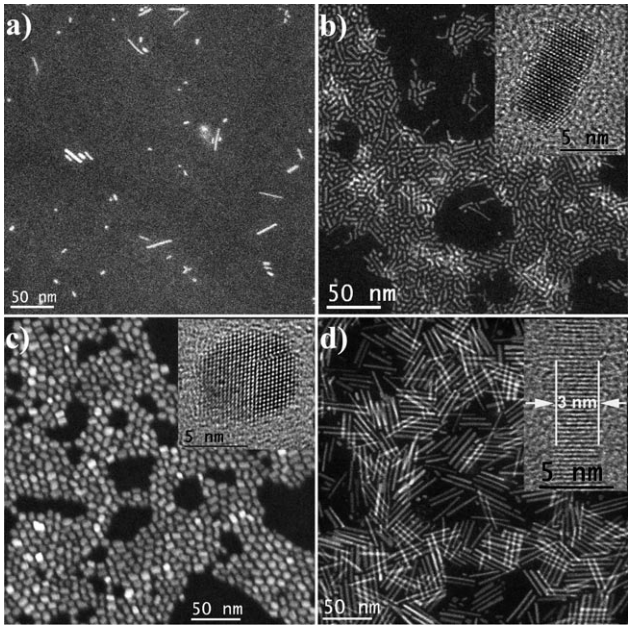

Figure 3. STEM images of different ZnS samples obtained by varying the experimental parameters used for magic-size NWs growth. a) Spherical nanocrystals and short nanorods grown without DDT. b) Short, branched, and wormlike nanorods grown with overdosed DDT (DDT:Zn = 30:1); c) Large spherical nanocrystals grown at increased temperature (at 260 °C). d) Long nanorods grown with overgrowth time. Insets in (b–d) show HRTEM images of the typical products.

Received: June 29, 2010
Revised: August 16, 2010
Published online: October 4, 2010

Keywords: colloids · nanowires · quantum chemistry · semiconductors · zinc

[1] P. D. Yang, R. X. Yan, M. Fardy, *Nano Lett.* **2010**, *10*, 1529.
[2] G. A. Ozin, L. Cademartiri, *Adv. Mater.* **2009**, *21*, 1013.

[3] Z. Li, Ö. Kurtulus, F. Nan, A. Myalitsin, Z. Wang, A. Kornowski, U. Pietsch, A. Mews, *Adv. Funct. Mater.* **2009**, *19*, 3650.
[4] J. Sun, W. E. Buhro, *Angew. Chem.* **2008**, *120*, 3259; *Angew. Chem. Int. Ed.* **2008**, *47*, 3215.
[5] L. Cademartiri, R. Malakooti, P. G. O'Brien, A. Migliori, S. Petrov, N. P. Kherani, G. A. Ozin, *Angew. Chem.* **2008**, *120*, 3874; *Angew. Chem. Int. Ed.* **2008**, *47*, 3814.
[6] N. Pradhan, H. Xu, X. Peng, *Nano Lett.* **2006**, *6*, 720.
[7] T. Yu, J. Joo, Y. I. Park, T. Hyeon, *J. Am. Chem. Soc.* **2006**, *128*, 1786.
[8] K. S. Cho, D. V. Talapin, W. Gaschler, C. B. Murray, *J. Am. Chem. Soc.* **2005**, *127*, 7140.
[9] Z. P. Liu, D. Xu, J. B. Liang, J. M. Shen, S. Y. Zhang, Y. T. Qian, *J. Phys. Chem. B* **2005**, *109*, 10699.
[10] T. Y. Yu, J. Joo, Y. I. Park, T. Hyeon, *Angew. Chem.* **2005**, *117*, 7577; *Angew. Chem. Int. Ed.* **2005**, *44*, 7411.
[11] A. B. Panda, S. Acharya, A. Efrima, *Adv. Mater.* **2005**, *17*, 2471.
[12] J. Li, L. W. Wang, *Chem. Mater.* **2004**, *16*, 4012.
[13] A. Kasuya, R. Sivamohan, Y. A. Barnakov, I. M. Dmitruk, T. Nirasawa, V. R. Romanyuk, V. Kumar, S. V. Mamykin, K. Tohji, B. Jeyadevan, K. Shinoda, T. Kudo, O. Terasaki, Z. Liu, R. V. Belosludov, V. Sundararajan, T. Kavazoe, *Nat. Mater.* **2004**, *3*, 99.
[14] M. J. Bowers II, J. R. McBride, S. J. Rosenthal, *J. Am. Chem. Soc.* **2005**, *127*, 15378.
[15] S. Kudera, M. Zanella, C. Giannini, A. Rizzo, Y. Q. Li, G. Gigli, R. Cingolani, G. Ciccarella, W. Spahl, W. J. Parak, L. Manna, *Adv. Mater.* **2007**, *19*, 548.
[16] Z. Deng, O. Schulz, S. Lin, B. Ding, X. Liu, X. Wei, R. Ros, H. Yan, Y. Liu, *J. Am. Chem. Soc.* **2010**, *132*, 5592.
[17] X. S. Fang, L. D. Zhang, *J. Mater. Sci. Technol.* **2006**, *22*, 721.
[18] D. Moore, Z. L. Wang, *J. Mater. Chem.* **2006**, *16*, 3898.
[19] Y. Jiang, X. M. Meng, J. Liu, Z. R. Hong, C. S. Lee, S. T. Lee, *Adv. Mater.* **2003**, *15*, 1195.
[20] J. Q. Hu, Y. Bando, J. H. Zhan, D. Golberg, *Adv. Funct. Mater.* **2005**, *15*, 757.
[21] X. S. Fang, C. H. Ye, L. D. Zhang, Y. H. Wang, Y. C. Wu, *Adv. Funct. Mater.* **2005**, *15*, 63.
[22] Y. Jiang, W. Zhang, J. Jie, X. Meng, J. Zapien, S. Lee, *Adv. Mater.* **2006**, *18*, 1527.
[23] X. S. Fang, Y. Bando, G. Z. Shen, C. H. Ye, U. K. Gautam, P. M. F. J. Costa, C. Y. Zhi, C. C. Tang, D. Golberg, *Adv. Mater.* **2007**, *19*, 2593.
[24] X. M. Meng, J. Liu, Y. Jiang, W. W. Chen, C. S. Lee, I. Bello, S. T. Lee, *Chem. Phys. Lett.* **2003**, *382*, 434.
[25] C. J. Barrelet, Y. Wu, D. C. Bell, C. M. Lieber, *J. Am. Chem. Soc.* **2003**, *125*, 11498.
[26] Z. Zhang, H. Yua, D. Liu, L. Liu, J. Shen, Y. Xiang, W. Ma, W. Zhou, S. Xie, *Nanotechnology* **2007**, *18*, 145607.
[27] J. H. Yu, J. Joo, H. M. Park, S. I. Baik, Y. W. Kim, S. C. Kim, T. Hyeon, *J. Am. Chem. Soc.* **2005**, *127*, 5662.
[28] Z. Deng, L. Cao, F. Tang, B. Zou, *J. Phys. Chem. B* **2005**, *109*, 16671.
[29] Z. Deng, H. Yan, Y. Liu, *J. Am. Chem. Soc.* **2009**, *131*, 17744.
[30] Y.-S. Fu, X.-W. Du, S. A. Kulnich, J.-S. Qiu, W.-J. Qin, R. Li, J. Sun, J. Liu, *J. Am. Chem. Soc.* **2007**, *129*, 16029.
[31] C. Schliehe, B. H. Juarez, M. Pelletier, S. Jander, D. Greshnykh, M. Nagel, A. Meyer, S. Foerster. A. Kornowski, C. Klinke, H. Weller, *Science* **2010**, *329*, 550.
[32] Z. A. Peng, X. Peng, *J. Am. Chem. Soc.* **2001**, *123*, 1389.

